

The Missing Massive Satellites of the Milky Way

Jie Wang^{1*}, Carlos Frenk¹, Julio F. Navarro², Liang Gao³ and Till Sawala¹

¹*Institute for Computational Cosmology, Department of Physics, University of Durham, South Road, Durham, DH1 3LE, UK*

²*Department of Physics and Astronomy, University of Victoria, PO Box 3055 STN CSC, Victoria, BC, V8W 3P6 Canada*

³*National Astronomical Observatories, Chinese Academy of Science, Beijing, 100012, China*

1 November 2018

ABSTRACT

Recent studies suggest that only three of the twelve brightest satellites of the Milky Way (MW) inhabit dark matter halos with maximum circular velocity, V_{\max} , exceeding ~ 30 km/s. This is in apparent contradiction with the Λ CDM simulations of the Aquarius Project, which suggest that MW-sized halos should have at least 8 subhalos with $V_{\max} > 30$ km/s. The absence of luminous satellites in such massive subhalos is thus puzzling and may present a challenge to the Λ CDM paradigm. We note, however, that the number of massive subhalos depends sensitively on the (poorly-known) virial mass of the Milky Way, and that their scarcity makes estimates of their abundance from a small simulation set like Aquarius uncertain. We use the Millennium Simulation series and the invariance of the scaled subhalo velocity function (i.e., the number of subhalos as a function of ν , the ratio of subhalo V_{\max} to host halo virial velocity, V_{200}) to secure improved estimates of the abundance of rare massive subsystems. In the range $0.1 < \nu < 0.5$, $N_{\text{sub}}(> \nu)$ is approximately Poisson-distributed about an average given by $\langle N_{\text{sub}} \rangle = 10.2 (\nu/0.15)^{-3.11}$. This is slightly lower than in Aquarius halos, but consistent with recent results from the Phoenix Project. The probability that a Λ CDM halo has 3 or fewer subhalos with V_{\max} above some threshold value, V_{th} , is then straightforward to compute. It decreases steeply both with decreasing V_{th} and with increasing halo mass. For $V_{\text{th}} = 30$ km/s, $\sim 40\%$ of $M_{\text{halo}} = 10^{12} M_{\odot}$ halos pass the test; fewer than $\sim 5\%$ do so for $M_{\text{halo}} \gtrsim 2 \times 10^{12} M_{\odot}$; and the probability effectively vanishes for $M_{\text{halo}} \gtrsim 3 \times 10^{12} M_{\odot}$. Rather than a failure of Λ CDM, the absence of massive subhalos might simply indicate that the Milky Way is less massive than is commonly thought.

Key words:

1 INTRODUCTION

The striking difference between the relatively flat faint-end slope of the galaxy stellar mass function and the much steeper cold dark matter halo mass function is usually reconciled by assuming that the efficiency of galaxy formation drops sharply with decreasing halo mass (see, e.g., White & Frenk 1991). Semi-analytic models of galaxy formation have used this result to explain the relatively small number of luminous satellites in the Milky Way (MW) halo, where Λ CDM simulations predict the existence of thousands of subhalos massive enough, in principle, to host dwarf galaxies. In these models, the small number of MW satellites reflects the relatively small number of subhalos massive enough to host luminous galaxies (see, e.g., Kauffmann et al. 1993; Bullock et al. 2000; Benson et al. 2002; Somerville

2002; Cooper et al. 2010; Li et al. 2010; Macciò et al. 2010; Guo et al. 2011; Font et al. 2011).

This is a model prediction that can be readily tested observationally, given the availability of radial velocity measurements for hundreds of stars in the dwarf spheroidal satellites of the Milky Way. Combined with photometric data, radial velocities tightly constrain the total mass enclosed within the luminous radius of these satellites (Walker et al. 2009; Wolf et al. 2010). The latter correlates strongly with the total dark mass of the dwarf, which is usually expressed in terms of its maximum circular velocity, V_{\max} , a quantity less affected than mass by tidal stripping (Peñarrubia et al. 2008).

Kinematical analyses of the Milky Way dwarf spheroidals have been attempted by several authors in recent years, with broad consensus on the results, at least for the best-studied nine brightest dwarf spheroidal MW companions: Draco, Ursa Minor, Fornax, Sculptor, Ca-

* Email: jie.wang@durham.ac.uk

rina, Leo I, Leo II, Canis Venatici I, and Sextans (see, e.g., Peñarrubia et al. 2008; Strigari et al. 2008; Lokas 2009; Walker et al. 2009; Wolf et al. 2010; Strigari et al. 2010). These studies suggest that some of these galaxies may inhabit halos with V_{\max} as low as 12 km/s, and agree that all¹ appear to inhabit halos with values of V_{\max} below a low threshold, $V_{\text{th}} \sim 30$ km/s. Only three dwarf irregular satellites – the Magellanic Clouds and the Sagittarius dwarf – may, in principle, inhabit halos exceeding this threshold.

The most straightforward interpretation of this result is that massive subhalos in the Milky Way are rare. However, as argued recently by Boylan-Kolchin et al. (2011, 2012), this is at odds with the results of the Aquarius Project, a series of N-body simulations of six different halos of virial² mass in the range $0.8 < M_{200}/10^{12} M_{\odot} < 1.8$. Boylan-Kolchin et al. (2011) noted that the largest subhalos in these simulations are significantly denser than inferred for the halos that host the brightest dwarf spheroidals in the Milky Way.

As discussed by Parry et al. (2012) and Boylan-Kolchin et al. (2012), the discrepancy can be traced to the fact that the largest Aquarius subhalos are significantly more massive or, equivalently, have too large a value of V_{\max} to be compatible with the measured kinematics of the brightest dwarf spheroidals. Specifically, the Aquarius halos have, on average, ~ 8 subhalos with $V_{\max} > 30$ km/s within the virial radius, larger than the V_{\max} of the brightest dwarf spheroidals, prompting questions about why these massive subhalos fail to host luminous satellites in the Milky Way. If this result holds, it may point to a failure of our basic understanding of how galaxies populate low mass halos or, more worryingly, of the Λ CDM paradigm itself.

Two issues may affect these conclusions. One is that the Aquarius Project simulation set contains only 6 halos and, therefore, estimates of the abundance of rare massive subhalos are subject to substantial uncertainty. The second point is that the number of massive subhalos is expected to depend sensitively on the virial mass of the host halo, which is only known to within a factor of 2-3 for the Milky Way.

We address these issues here by using large numbers of well-resolved halos identified in the Millennium Simulation series (Springel et al. 2005; Boylan-Kolchin et al. 2009). This is possible because, in agreement with earlier work, we find that the abundance of subhalos, when scaled appropriately, is independent of halo mass (see, e.g., Moore et al. 1999; Kravtsov et al. 2004; Springel et al. 2008). We use this to derive improved estimates of the average number of massive subhalos, as well as its statistical distribution. The probability that a halo has as few massive subhalos as the Milky Way can then be evaluated, both as a function of host halo mass and/or subhalo mass threshold.

This paper is organized as follows. Sec. 2 describes briefly the simulations we used in our analysis. We present

¹ One possible exception is Draco, where the data might allow a more massive halo.

² Unless otherwise noted, we define virial quantities as those corresponding to spheres that enclose a mean overdensity $\Delta = 200$ times the critical density for closure. M_{200} , for example, corresponds to the mass within the virial radius, r_{200} . When other values of Δ are assumed the subscript is adjusted accordingly.

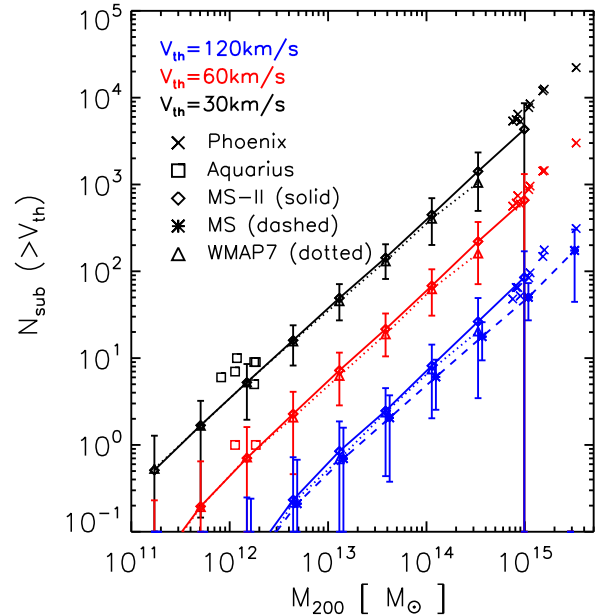


Figure 1. The number of subhaloes with $V_{\max} \geq V_{\text{th}}$ as a function of the virial mass of their host haloes, M_{200} , in the Millennium Simulations (MS and MS-II), as well as in the level-2 runs of the Aquarius and Phoenix Projects. Subhaloes are identified within the virial radius, r_{200} , of their host systems. Different symbols correspond to each simulation, as labelled, and are coloured according to the value of the threshold, V_{th} . Error bars denote the rms plus Poisson error in each mass bin. Note the nearly linear dependence of the number of subhaloes with halo mass. Due to numerical resolution, few subhaloes with velocities less than ~ 100 km/s are found in the MS simulation, so the $V_{\text{th}} = 30$ and 60 km/s MS curves in this case are omitted for clarity. For massive, well-resolved halos the results are much less affected by numerical limitations and there is good agreement between MS and MS-II. Subhalo abundance is insensitive to small variations in the cosmological parameters. Triangles connected by a dotted line show results corresponding to a run that adopted the latest WMAP7 parameters (Komatsu et al. 2011); in contrast, the Millennium Simulations adopted parameters consistent with the 1st-year analysis of WMAP data.

our main results in Sec. 3, and end with a brief summary in Sec. 4.

2 SIMULATIONS

The two Millennium simulations (MS; Springel et al. 2005 and MS-II; Boylan-Kolchin et al. 2009) provide the main datasets used in this study. Both are simulations of a flat WMAP-1 Λ CDM cosmogony with the following parameters: $\Omega_M = 0.25$, $\Omega_b = 0.045$, $h = 0.73$, $n_s = 1$ and $\sigma_8 = 0.9$.

The MS run evolved a box 500 Mpc/h on a side, with 2160^3 particles of mass $m_p = 8.6 \times 10^8 M_{\odot}/h$. MS-II evolved the same total number of particles in a box 1/125 the volume of MS and had, therefore, 125 better mass resolution ($m_p = 6.885 \times 10^6 M_{\odot}/h$). The nominal spatial resolution is given by the Plummer-equivalent gravitational softening, which is

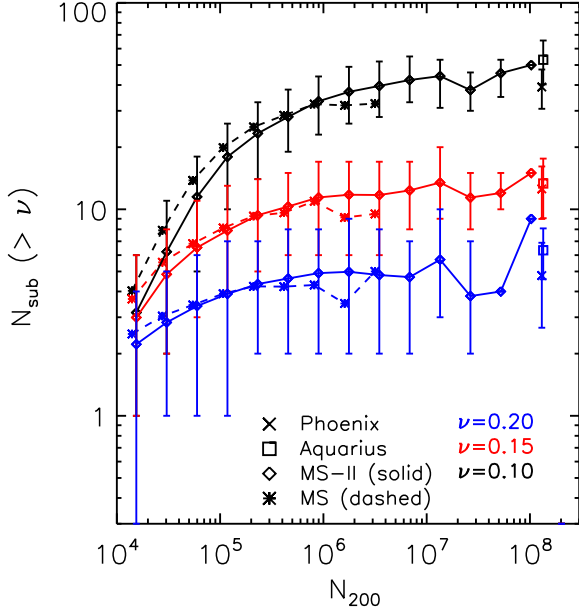


Figure 2. The number of subhalos with maximum circular velocity exceeding a certain fraction, ν , of their host halo virial velocity, as a function of N_{200} , the number of particles within the virial radius of the host. Curves for three values of $\nu = 0.1, 0.15,$ and 0.2 are shown. Error bars for MS and MS-II indicate the 10 and 90 percentile in each bin, and are omitted when the bin contains a single halo. The excellent agreement between results for MS and MS-II at given N_{200} reflects the halo mass invariance of the $N_{\text{sub}}(> \nu)$ function; each particle is $125\times$ more massive in MS than in MS-II. Results converge for well-resolved halos (i.e., those with large N_{200}). As expected, the smaller ν the larger the minimum number of particles, N_{200}^{min} , needed to obtain converged results.

$\epsilon_P = 5 \text{ kpc}/h$, and $1 \text{ kpc}/h$ for the MS and MS-II runs, respectively.

We also use halos from the Aquarius Project (Springel et al. 2008) and the Phoenix Project (Gao et al. 2012) (level-2 resolution). These are ultra high-resolution simulations of six MW-sized halos ($M_{200} \sim 10^{12} M_\odot$) and nine cluster-sized halos ($M_{200} \sim 10^{15} M_\odot$), each resolved with a few hundred million particles within the virial radius.

The normalization of the power spectrum adopted in these simulations is slightly higher than favoured by the latest WMAP dataset (WMAP7; Komatsu et al. 2011), but this is expected to affect the abundance of halos of given virial mass rather than the mass function of subhalos, which is the main focus of our study. We have verified this explicitly by analyzing a 1620^3 -particle simulation of a $70.4 \text{ Mpc}/h$ box that adopts the WMAP7 cosmological parameters (see Fig. 1). The particle mass in this run is $6.20 \times 10^6 M_\odot/h$ and gravitational interactions were softened with $\epsilon_P = 1 \text{ kpc}/h$.

Halos and subhalos are identified in all simulations by SUBFIND (Springel et al. 2001), a recursive algorithm that identifies self-bound structures and substructures in N-body simulations.

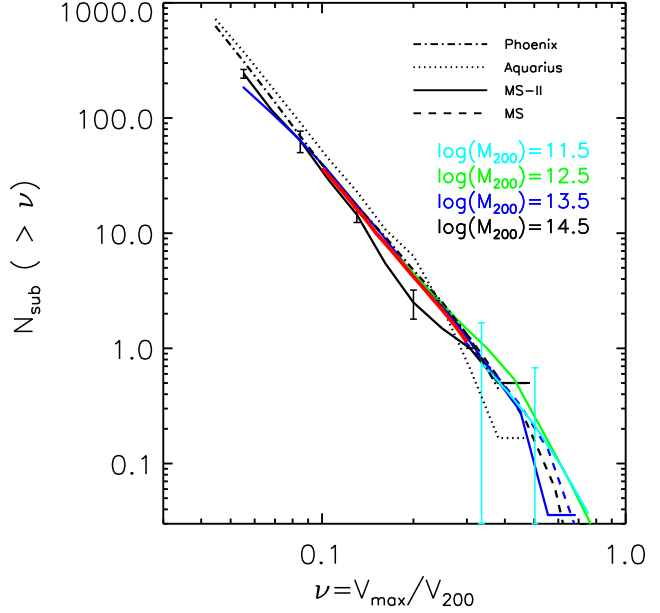


Figure 3. The scaled subhalo velocity function, i.e., the number of subhalos with maximum circular velocity exceeding a certain fraction, $\nu = V_{\text{max}}/V_{200}$, of the host halo virial velocity. Dotted and dot-dashed curves show averages for the six Aquarius halos and nine Phoenix halos, respectively. Dashed and solid curves correspond to MS and MS-II. Four curves are shown for each, corresponding to averages over all halos in mass bins of width 0.1 dex centred at $\log_{10} M_{200}/M_\odot = 11.5, 12.5, 13.5,$ and 14.5 . Error bars (shown only for the lowest and highest mass bins) indicate the *rms* scatter in each bin. Only halos satisfying the constraint $N_{200} > N_{200}^{\text{min}}(\nu)$ are used. All simulations are in good agreement when well-resolved halos are considered. The scaled subhalo velocity function is thus nearly invariant with mass. See text for further discussion.

3 RESULTS

We first investigate the scale invariance and other statistical properties of the distribution of subhalo V_{max} and then apply our results to subhalos in the Milky Way.

3.1 Subhalo V_{max} distribution

Fig. 1 shows, as a function of host halo virial mass, the total number³ of subhalos with maximum circular velocity, V_{max} , exceeding a specified velocity threshold, V_{th} . Results are shown for three different values of V_{th} . The average number of subhalos in each halo mass bin is shown by symbols connected by solid (MS-II) or dashed (MS) lines. Individual level-2 Phoenix and Aquarius halos are shown by crosses and open squares, respectively. WMAP7 results are shown by open triangles connected by a dotted line.

Fig. 1 illustrates that: (i) the number of subhalos depends roughly linearly on halo mass and increases strongly with decreasing velocity threshold, and that (ii)

³ Unless otherwise noted, we identify subhalos within the virial radius, r_{200} , of the host halo.

the slight change in cosmological parameters from WMAP1 to WMAP7 has a negligible effect on subhalo abundance.

Fig. 1 also shows that numerical resolution limits the halo mass and velocity threshold for which convergence in subhalo abundances is achieved. Indeed, there are fewer subhalos in MS, the simulation with poorest mass resolution; so few with velocities less than ~ 100 km/s that the $V_{\text{th}} = 30$ and 60 km/s MS curves have been omitted for clarity. When halos and subhalos are resolved with enough particles, however, the results converge well. For $V_{\text{th}} = 120$ km/s, MS, MS-II, and WMAP7 halos yield similar numbers of subhalos over the whole halo mass range considered, despite the fact that, at given M_{200} , MS-II and WMAP7 halos have $\sim 125\times$ more particles than their MS counterparts. Furthermore, the results for Phoenix and Aquarius are in good agreement with MS-II, even though halos in MS-II have $700\times$ fewer particles than Phoenix and $2\times$ fewer particles than Aquarius, respectively.

We explore the requirements for numerical convergence in more detail in Fig. 2, where we plot, as a function of the total number of particles within the virial radius, N_{200} , the average number of subhalos with V_{max} exceeding a certain fraction of the host halo virial velocity: $N_{\text{sub}}(> \nu)$, for $\nu = V_{\text{max}}/V_{200} = 0.10, 0.15$, and 0.20 . Results are shown for MS and MS-II halos with dashed and solid curves, respectively.

This figure highlights two important points. One is that at given ν there is good agreement between all simulations provided that halos are resolved with enough particles. The second is that, when the first condition is met, $N_{\text{sub}}(> \nu)$ is independent of halo mass. (Recall that, at fixed N_{200} , MS halos are $125\times$ more massive than their MS-II counterparts.) This agreement, together with the fact that the $N_{\text{sub}}(> \nu)$ curves plateau at large values of N_{200} , imply that the *scaled* subhalo velocity function (i.e., the number of subhalos as a function of $\nu = V_{\text{max}}/V_{200}$) is invariant over many decades in halo mass. Fig. 2 also makes clear that numerical convergence requires that a halo be resolved with a total number of particles above some (ν -dependent) minimum number, N_{200}^{min} (listed in Table 1). The converged values agree well, within the statistical uncertainty, with the results for Phoenix and Aquarius halos.

We show the invariance of subhalo abundance explicitly in Fig. 3, where $N_{\text{sub}}(> \nu)$ is plotted for MS and MS-II halos grouped in 4 bins of different halo mass. Only halos satisfying the $N_{200} > N_{200}^{\text{min}}$ constraint are used here. These results confirm earlier work (see, e.g., Moore et al. 1999; Kravtsov et al. 2004; Zheng et al. 2005; Weinberg et al. 2008; Springel et al. 2008), and imply that we can combine all well-resolved halos into one large sample to derive robust estimates of the statistical *distribution* of $N_{\text{sub}}(> \nu)$.

This is shown in Fig. 4 for $\nu = 0.1, 0.15$, and 0.2 , computed using all MS and MS-II halos with $N_{200} > N_{200}^{\text{min}}(\nu)$, as given in Table 1. In the top panel, which corresponds to subhalos identified within r_{200} , the histograms show the $N_{\text{sub}}(> \nu)$ distributions for the 614, 3070, and 6867 halos that satisfy, respectively, the minimum particle number constraint. The bottom panel shows subhalo numbers identified within a slightly larger radius, r_{100} , which is on average $\sim 30\%$ larger than r_{200} . (The mean and rms dispersion of the distributions of $N_{\text{sub}}(> \nu)$ are listed in Table 1.) Note that the results obtained for MS and MS-II

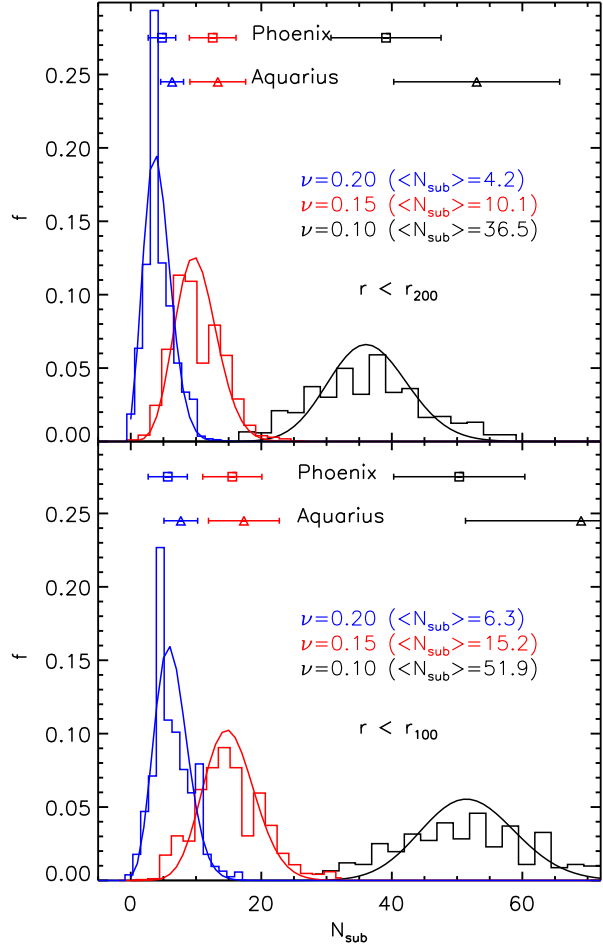


Figure 4. The distribution of $N_{\text{sub}}(> \nu)$ for $\nu = 0.1, 0.15$, and 0.2 , computed for well-resolved MS and MS-II halos; i.e., those with particle numbers exceeding $N_{200}^{\text{min}}(\nu)$ (as given in Table 1). The top panel refers to all subhalos within the virial radius, r_{200} ; the bottom panel to subhalos within a radius roughly 30% larger, r_{100} . The average and rms for Aquarius and Phoenix halos are shown at the top of the plot. Note that subhalos in Aquarius seem slightly overabundant relative to either Phoenix or the Millennium Simulations, but still well within the statistical uncertainty. The $N_{\text{sub}}(> \nu)$ distribution is well approximated by a Poisson distribution: the solid curves show Poisson distributions with the same averages as each histogram.

are in excellent agreement with the results obtained for Phoenix halos. Subhalos in Aquarius are slightly overabundant, perhaps because of small biases in their assembly histories (Boylan-Kolchin et al. 2010), but still consistent with the MS and MS-II results given the large variance ($\sigma_{N_{\text{sub}}}^2$) expected from the sample of only 6 Aquarius halos. Note as well that, as expected, the larger volume encompassed by r_{100} yields larger subhalo numbers than found when identifying subhalos only within r_{200} . For $r < r_{200}$, the average

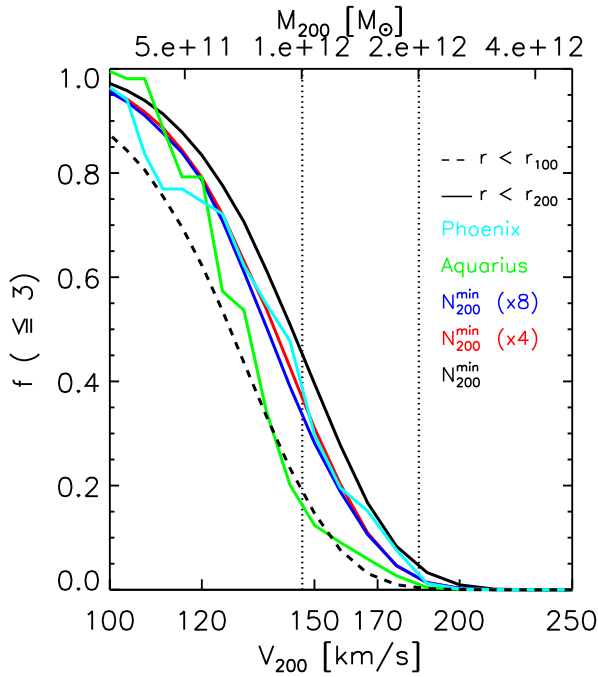


Figure 5. Probability that a halo contains 3 or fewer subhalos with $V_{\max} > 30$ km/s, as a function of halo mass (top tickmarks) or virial velocity (bottom tickmarks). The solid black curve corresponds to assuming Poisson statistics and that $N_{\text{sub}}(> \nu) = 10.2(\nu/0.15)^{-3.11}$, the average number of subhalos within the virial radius of well-resolved MS and MS-II halos with particle numbers exceeding N_{200}^{\min} (see Table 1). The sensitivity of the result to the assumed minimum number of particles is shown by the red and blue curves, which correspond to increasing the values of $N_{200}^{\min}(\nu)$ by factors of 4 or 8, respectively. Results using only the nine Phoenix or six Aquarius halos are shown in cyan and green, respectively. Note that because subhalos are slightly overabundant in Aquarius (see Fig. 4) the probabilities are systematically lower than when considering either Phoenix halos or the Millennium simulations. The same is true if subhalos are identified within a radius larger than the virial radius. The dashed curve shows probabilities when the search radius around each halo is increased by roughly 30% to r_{100} .

$N_{\text{sub}}(> \nu)$ is a steep function of ν , well approximated, in the range $0.1 < \nu < 0.5$, by

$$\langle N_{\text{sub}} \rangle (> \nu) = 10.2(\nu/0.15)^{-3.11}. \quad (1)$$

Fig. 4 also shows that the distribution of $N_{\text{sub}}(> \nu)$ follows Poisson statistics closely; the solid curves are actually *not* fits, but just Poisson distributions with the same average as each of the histograms. Clearly, these provide a good description of the distribution of $N_{\text{sub}}(> \nu)$ at fixed ν . This conclusion is supported by earlier work (see, e.g., Kravtsov et al. 2004; Boylan-Kolchin et al. 2010), as well as by the data listed in Table 1: the average number of subhalos is roughly similar to the variance, as expected from a Poisson process.

3.2 Massive satellites in the Milky Way

We can use these results to address the Milky Way missing massive satellites problem highlighted in Sec. 1. In particu-

lar, it is straightforward to compute the probability that a halo has X or fewer subhalos with $V_{\max} > 30$ km/s within its virial radius, once a virial mass (or, equivalently, a virial velocity, V_{200}) has been assumed for the Milky Way. This is given by,

$$f(\leq X) = \sum_{k=0}^X \frac{\lambda_\nu^k}{k!} e^{-\lambda_\nu}, \quad (2)$$

where $\lambda_\nu = \langle N_{\text{sub}} \rangle (> \nu)$ is given by Eqn. 1.

The solid black curve in Fig. 5 shows $f(\leq 3)$ as a function of virial mass (upper tickmarks on the abscissa) or virial velocity (lower tickmarks). The probability is a steep function of the assumed halo mass: more than 40% of $10^{12} M_\odot$ halos pass this test, but only $\sim 5\%$ of $2 \times 10^{12} M_\odot$ systems do so. The probability becomes negligible for $M_{200} \gtrsim 3 \times 10^{12} M_\odot$. This suggests that the scarcity of massive subhalos is best thought of as placing a strong upper limit on the virial mass of the Milky Way, rather than as a failure of the Λ CDM scenario.

It is important to assess the sensitivity of this conclusion to the parameters assumed in this study. For example, should the velocity threshold be placed at 25 km/s, rather than at 30 km/s, as argued by Boylan-Kolchin et al. (2012), the upper limit on the mass of the Milky Way would become even more restrictive. The results, however, could still be read from Fig. 5, after shifting the tickmarks by $30/25 = 1.2$ in the velocity axis or by $1.2^3 = 1.73$ in the mass axis. Thus, for $V_{\text{th}} = 25$ km/s, a probability of more than 5% requires a halo mass $M_{200} < 1 \times 10^{12} M_\odot$, rather than the $M_{200} < 2 \times 10^{12} M_\odot$ appropriate to $V_{\text{th}} = 30$ km/s.

We have also examined the dependence of our results on $N_{200}^{\min}(\nu)$, the assumed minimum number of particles needed for convergence (listed in Table 1). This is shown by the red and blue curves in Fig. 5, which correspond to increasing N_{200}^{\min} by a factor of 4 and 8, respectively, before deriving $\langle N_{\text{sub}} \rangle (> \nu)$. Fig. 5 makes clear that our results are quite insensitive to such changes in N_{200}^{\min} .

Since Phoenix halos have subhalo abundances in good agreement with those in Eqn. 1, our results would not change had we chosen the nine Phoenix halos to compute $\langle N_{\text{sub}} \rangle (> \nu)$ (see cyan curve in Fig. 5). On the other hand, had we chosen to derive $\langle N_{\text{sub}} \rangle (> \nu)$ solely from the six Aquarius halos, the slight overabundance of subhalos in these systems would lead to stricter upper limits on the Milky Way halo mass, as shown by the green curve in Fig. 5. This result, together with the fact that the average Aquarius halo mass ($1.42 \times 10^{12} M_\odot$) is uncomfortably close to the upper limit discussed above is apparently the reason why Boylan-Kolchin et al. (2011) originally found such a strong discrepancy between the Aquarius simulations and the Milky Way.

Finally, we need to consider the dependence of the number of subhalos on the maximum radius used to identify substructure. The results discussed above refer to subhalos identified within the virial radius, r_{200} , which is ~ 200 kpc for a $M_{200} = 10^{12} M_\odot$ halo. This is smaller than the maximum distance commonly adopted to identify dwarf galaxies as Milky Way satellites; for example, Leo I is at roughly 250 kpc from the centre of the Galaxy. Therefore, it might be argued that subhalos should be counted within a larger radius in order to make a meaningful comparison. As shown in the bot-

tom panel of Fig. 4, subhalos are roughly $\sim 50\%$ more abundant within r_{100} than within r_{200} . For a $M_{200} = 10^{12} M_{\odot}$ halo, $r_{100} \approx 270$ kpc, comparable to the Galactocentric distance of Leo I. In analogy with Eqn. 1, the average number of subhalos, $N_{\text{sub}}(> \nu)$, within r_{100} is well approximated, in the range $0.1 < \nu < 0.5$, by

$$\langle N_{\text{sub}} \rangle (> \nu) = 15.03 (\nu/0.15)^{-3.06}. \quad (3)$$

The dashed line in Fig. 5 shows that the probability of hosting at most 3 massive subhalos drops significantly when the r_{100} radius is used; only about 20% of $M_{200} = 10^{12} M_{\odot}$ halos pass the test then. This stricter constraint emphasizes the difficulty of resolving the missing massive satellite problem if the Milky Way mass significantly exceeds $10^{12} M_{\odot}$.

4 SUMMARY

We have used the Millennium Simulation series, together with the ultra-high resolution simulations of small halo samples from the Aquarius and Phoenix projects to study the abundance of rare, massive subhalos in Λ CDM halos. As in earlier work, we find that the scaled subhalo velocity function (i.e., the number of subhalos as a function of the ratio between subhalo maximum circular velocity and host halo virial velocity, $\nu = V_{\text{max}}/V_{200}$) is independent of halo mass. This implies that we can obtain robust estimates of the statistical distribution of massive subhalos from large samples of well-resolved halos selected from the Millennium simulations.

Our main result is that, in the range $0.1 < \nu < 0.5$, the number of subhalos within the virial radius, r_{200} , is Poisson-distributed around an average given by Eqn. 1. Compared to this average, subhalos in the Aquarius Project are slightly overabundant but still consistent given the large variance and the small sample of halos included in that simulation suite. Subhalos in the cluster-sized Phoenix Project halos are in excellent agreement with Eqn. 1.

We have then used this result to compute the probability that a halo of virial velocity V_{200} has a certain number of massive subhalos with V_{max} exceeding a velocity threshold, V_{th} . Applied to the Milky Way, where observations suggest that no more than 3 (or at most 4) subhalos with $V_{\text{max}} > 30$ km/s host luminous satellites, we find that this constraint effectively translates into a strong upper limit on the Milky Way halo mass. The probability that a halo with $M_{200} \gtrsim 3 \times 10^{12} M_{\odot}$ satisfies this constraint within radius r_{200} is vanishingly small, but it increases rapidly with decreasing virial mass. Roughly 45% of $M_{200} = 10^{12} M_{\odot}$ halos pass this test, and $\sim 90\%$ of all halos with $M_{200} \sim 5 \times 10^{11} M_{\odot}$ are consistent with the data. These fractions are reduced to $\sim 20\%$ and $\sim 70\%$, respectively, if subhalos are considered within a larger search radius, $r_{100} \sim 1.3 r_{200}$ (which, for halos of mass $\sim 10^{12} M_{\odot}$, is close to the Galactocentric distance of Leo I, the most distant bright satellite known in the Milky Way). In this case, the number of subhalos, $\langle N_{\text{sub}} \rangle (> \nu)$, within r_{100} is given by Eqn. 3 and a Milky Way halo mass of $M_{200} = 2 \times 10^{12} M_{\odot}$ is strongly ruled out by the satellite data.

The ‘‘missing massive satellites problem’’ in the Milky Way halo highlighted by Boylan-Kolchin et al. (2011, 2012) and by Parry et al. (2012) may thus be resolved if the

mass of the Milky Way halo is $\sim 10^{12} M_{\odot}$ (see also Vera-Ciro et al. 2012). This is well within the range of halo masses allowed by the latest estimates based on either the timing argument (Li & White 2008) or on abundance-matching methods (Guo et al. 2010). It is in even better agreement with the lower virial masses reported by estimates based on (i) the radial velocity dispersion of Milky Way satellites and halo stars (Battaglia et al. 2005; Sales et al. 2007); (ii) the escape speed in the solar neighbourhood (Smith et al. 2007); or (iii) the kinematics of halo blue horizontal branch stars (Xue et al. 2008). Invoking a $\sim 10^{12} M_{\odot}$ mass for the Milky Way is a simpler and more straightforward resolution than several alternatives advanced in recent papers, such as considering the baryon adiabatic contraction and feedback (di Cintio et al. 2011), reducing the central density of subhalos through tidal stripping (Di Cintio et al. 2012; Vera-Ciro et al. 2012), or positing radical revisions to the nature of dark matter (Lovell et al. 2012; Vogelsberger et al. 2012).

We conclude that there is no compelling requirement to revise the Λ CDM paradigm based on the abundance of massive subhalos in the Milky Way. There are still, however, some uncomfortable corollaries to this solution. One is that a $10^{12} M_{\odot}$ halo has a virial velocity of only ~ 150 km/s, well below the rotation speed of the Milky Way disk, usually assumed to be $V_{\text{rot}} = 220$ km/s, or even higher (Reid et al. 2009). This seems at odds with results from some semi-analytic models of galaxy formation that attempt simultaneously to match the Tully-Fisher relation and the galaxy stellar mass function: agreement with observation seems to require $V_{\text{rot}} \approx V_{200}$ (see, e.g., Cole et al. 2000; Croton et al. 2006).

A further worry is that an $M_{200} = 10^{12} M_{\odot}$ halo might not be massive enough to host satellites as massive as the Magellanic Clouds. Assuming that V_{max} for the LMC and SMC can be identified with the rotation speed of their HI disks, or 60 and 50 km/s, respectively (Kim et al. 1998; Stanimirović et al. 2004), we find, using the data in Table 1, that only $\sim 62\%$ of $V_{200} = 150$ km/s halos would be expected not to host an LMC-like system. The probability of hosting two (or more) subhalos more massive than the SMC is of order 20%. None of these probabilities seem unlikely enough to cause worry.

Although our results may explain why few massive subhalos might be expected in the Milky Way halo, this explanation still assigns MW satellites to very low mass halos, i.e., those with $V_{\text{max}} < 30$ km/s. These halos have masses below $10^{10} M_{\odot}$, the mass scale below which semi-analytic models predict that galaxy formation efficiency should become exceedingly small (Guo et al. 2010). Given the large number of low mass halos expected in a Λ CDM universe, populating even a small fraction of $V_{\text{max}} < 30$ km/s systems with galaxies as bright as Fornax might lead to substantially overpredicting the number of dwarfs in the local Universe (see, e.g., Ferrero et al. 2011). Without a full accounting of how dwarf galaxies form in low-mass halos, concerns about the viability of Λ CDM on small scales will be hard to dispel.

Table 1. $N_{200}^{\min}(\nu)$ is the minimum number of particles within the virial radius of a halo needed to achieve convergence in the abundance of subhalos. N_{halos} is the number of halos that satisfy such condition in the Millennium Simulations. $\langle N_{\text{sub}} \rangle$ and $\sigma_{N_{\text{sub}}}$ are the average number of subhalos exceeding ν and its dispersion, respectively.

| ν (V_{max}/V_{200}) | 0.1 | 0.15 | 0.2 | 0.25 | 0.3 | 0.35 | 0.4 | 0.45 | 0.5 |
|--|-------------------|-------------------|-------------------|-------------------|-------------------|-------------------|-------------------|-------------------|-------------------|
| N_{200}^{\min} | 1.0×10^6 | 2.5×10^5 | 1.2×10^5 | 7.5×10^4 | 2.5×10^4 | 1.8×10^4 | 1.0×10^4 | 7.5×10^3 | 5.0×10^3 |
| N_{halos} | 614 | 3070 | 6867 | 12138 | 38550 | 54568 | 90200 | 113585 | 151663 |
| $\langle N_{\text{sub}} \rangle (r < r_{200})$ | 36.55 | 10.14 | 4.20 | 2.12 | 1.14 | 0.71 | 0.48 | 0.34 | 0.25 |
| $\sigma_{N_{\text{sub}}} (r < r_{200})$ | 8.92 | 3.87 | 2.27 | 1.54 | 1.10 | 0.85 | 0.68 | 0.57 | 0.48 |
| $\langle N_{\text{sub}} \rangle (r < r_{100})$ | 51.91 | 15.22 | 6.3 | 3.11 | 1.73 | 1.06 | 0.69 | 0.46 | 0.33 |
| $\sigma_{N_{\text{sub}}} (r < r_{100})$ | 12.2 | 5.23 | 2.99 | 1.98 | 1.39 | 1.08 | 0.84 | 0.68 | 0.58 |

ACKNOWLEDGEMENTS

We thank Mike Boylan-Kolchin, Volker Springel and Simon White for useful suggestions and comments on early versions of this work. We also thank an anonymous referee for helpful comments which helped improve this paper. The simulations analyzed in this paper were carried out by the Virgo consortium for cosmological simulations and we are grateful to our consortium colleagues for permission to use the data. Some of the calculations were performed on the DiRAC facility jointly funded by STFC, the Large Facilities Capital Fund of the department for Business, Innovation and Skills and Durham University. JW acknowledges a Royal Society Newton International Fellowship and CSF a Royal Society Wolfson Research Merit Award This work was supported by ERC Advanced Investigator grant COSMIWAY and an STFC rolling grant to the Institute for Computational Cosmology. LG acknowledges support from the one-hundred-talents program of the Chinese academy of science (CAS), MPG partner Group family, the National Basic Research Program of China (program 973 under grant No. 2009CB24901), NSFC grants (Nos. 10973018 and 11133003) and an STFC Advanced Fellowship, as well as the hospitality of the Institute for Computational Cosmology at Durham University.

REFERENCES

Battaglia G., Helmi A., Morrison H., Harding P., Olszewski E. W., Mateo M., Freeman K. C., Norris J., Shtetman S. A., 2005, *MNRAS*, 364, 433
 Benson A. J., Lacey C. G., Baugh C. M., Cole S., Frenk C. S., 2002, *MNRAS*, 333, 156
 Boylan-Kolchin M., Bullock J. S., Kaplinghat M., 2011, *MNRAS*, 415, L40
 Boylan-Kolchin M., Bullock J. S., Kaplinghat M., 2012, *MNRAS*, p. 2657
 Boylan-Kolchin M., Springel V., White S. D. M., Jenkins A., 2010, *MNRAS*, 406, 896
 Boylan-Kolchin M., Springel V., White S. D. M., Jenkins A., Lemson G., 2009, *MNRAS*, 398, 1150
 Bullock J. S., Kravtsov A. V., Weinberg D. H., 2000, *ApJ*, 539, 517
 Cole S., Lacey C. G., Baugh C. M., Frenk C. S., 2000, *MNRAS*, 319, 168

Cooper A. P., Cole S., Frenk C. S., White S. D. M., Helly J., Benson A. J., De Lucia G., Helmi A., Jenkins A., Navarro J. F., Springel V., Wang J., 2010, *MNRAS*, 406, 744
 Croton D. J., Springel V., White S. D. M., De Lucia G., Frenk C. S., Gao L., Jenkins A., Kauffmann G., Navarro J. F., Yoshida N., 2006, *MNRAS*, 365, 11
 Di Cintio A., Knebe A., Libeskind N. I., Brook C., Yepes G., Gottloeber S., Hoffman Y., 2012, *ArXiv e-prints*
 di Cintio A., Knebe A., Libeskind N. I., Yepes G., Gottlöber S., Hoffman Y., 2011, *MNRAS*, 417, L74
 Ferrero I., Abadi M. G., Navarro J. F., Sales L. V., Gurovich S., 2011, *ArXiv e-prints*
 Font A. S., Benson A. J., Bower R. G., Frenk C. S., Cooper A., De Lucia G., Helly J. C., Helmi A., Li Y.-S., McCarthy I. G., Navarro J. F., Springel V., Starkeburg E., Wang J., White S. D. M., 2011, *MNRAS*, 417, 1260
 Gao L., Navarro J. F., Frenk C. S., Jenkins A., Springel V., White S. D. M., 2012, *ArXiv e-prints*
 Guo Q., White S., Boylan-Kolchin M., De Lucia G., Kauffmann G., Lemson G., Li C., Springel V., Weinmann S., 2011, *MNRAS*, 413, 101
 Guo Q., White S., Li C., Boylan-Kolchin M., 2010, *MNRAS*, pp 367–376
 Kauffmann G., White S. D. M., Guiderdoni B., 1993, *MNRAS*, 264, 201
 Kim S., Staveley-Smith L., Dopita M. A., Freeman K. C., Sault R. J., Kesteven M. J., McConnell D., 1998, *ApJ*, 503, 674
 Komatsu E., Smith K. M., Dunkley J., Bennett C. L., Gold B., Hinshaw G., Jarosik N., Larson D., Nolte M. R., Page L., Spergel D. N., et al. 2011, *ApJS*, 192, 18
 Kravtsov A. V., Berlind A. A., Wechsler R. H., Klypin A. A., Gottlöber S., Allgood B., Primack J. R., 2004, *ApJ*, 609, 35
 Li Y.-S., De Lucia G., Helmi A., 2010, *MNRAS*, 401, 2036
 Li Y.-S., White S. D. M., 2008, *MNRAS*, 384, 1459
 Lokas E. L., 2009, *MNRAS*, 394, L102
 Lovell M. R., Eke V., Frenk C. S., Gao L., Jenkins A., Theuns T., Wang J., White S. D. M., Boyarsky A., Ruchayskiy O., 2012, *MNRAS*, 420, 2318
 Macciò A. V., Kang X., Fontanot F., Somerville R. S., Koposov S., Monaco P., 2010, *MNRAS*, 402, 1995
 Moore B., Ghigna S., Governato F., Lake G., Quinn T., Stadel J., Tozzi P., 1999, *ApJ*, 524, L19
 Parry O. H., Eke V. R., Frenk C. S., Okamoto T., 2012, *MNRAS*, 419, 3304

- Peñarrubia J., McConnachie A. W., Navarro J. F., 2008, *ApJ*, 672, 904
- Peñarrubia J., Navarro J. F., McConnachie A. W., 2008, *ApJ*, 673, 226
- Reid M. J., Menten K. M., Zheng X. W., Brunthaler A., Moscadelli L., Xu Y., Zhang B., Sato M., Honma M., Hirota T., Hachisuka K., Choi Y. K., Moellenbrock G. A., Bartkiewicz A., 2009, *ApJ*, 700, 137
- Sales L. V., Navarro J. F., Abadi M. G., Steinmetz M., 2007, *MNRAS*, 379, 1464
- Smith M. C., X. et al. 2007, *MNRAS*, 379, 755
- Somerville R. S., 2002, *ApJ*, 572, L23
- Springel V., Wang J., Vogelsberger M., Ludlow A., Jenkins A., Helmi A., Navarro J. F., Frenk C. S., White S. D. M., 2008, *MNRAS*, 391, 1685
- Springel V., White S. D. M., Jenkins A., Frenk C. S., Yoshida N., Gao L., Navarro J., Thacker R., Croton D., Helly J., Peacock J. A., Cole S., Thomas P., Couchman H., Evrard A., Colberg J., Pearce F., 2005, *Nature*, 435, 629
- Springel V., Yoshida N., White S. D. M., 2001, *New Astronomy*, 6, 79
- Stanimirović S., Staveley-Smith L., Jones P. A., 2004, *ApJ*, 604, 176
- Strigari L. E., Bullock J. S., Kaplinghat M., Simon J. D., Geha M., Willman B., Walker M. G., 2008, *Nature*, 454, 1096
- Strigari L. E., Frenk C. S., White S. D. M., 2010, *MNRAS*, 408, 2364
- Vera-Ciro C. A., Helmi A., Starkenburg E., Breddels M. A., 2012, *ArXiv e-prints*
- Vogelsberger M., Zavala J., Loeb A., 2012, *ArXiv e-prints*
- Walker M. G., Mateo M., Olszewski E. W., Peñarrubia J., Wyn Evans N., Gilmore G., 2009, *ApJ*, 704, 1274
- Weinberg D. H., Colombi S., Davé R., Katz N., 2008, *ApJ*, 678, 6
- White S. D. M., Frenk C. S., 1991, *ApJ*, 379, 52
- Wolf J., Martinez G. D., Bullock J. S., Kaplinghat M., Geha M., Muñoz R. R., Simon J. D., Avedo F. F., 2010, *MNRAS*, 406, 1220
- Xue X. X., Rix H. W., Zhao G., Re Fiorentin P., Naab T., Steinmetz M., van den Bosch F. C., Beers T. C., Lee Y. S., Bell E. F., Rockosi C., Yanny B., Newberg H., Wilhelm R., Kang X., Smith M. C., Schneider D. P., 2008, *ApJ*, 684, 1143
- Zheng Z., Berlind A. A., Weinberg D. H., Benson A. J., Baugh C. M., Cole S., Davé R., Frenk C. S., Katz N., Lacey C. G., 2005, *ApJ*, 633, 791

This paper has been typeset from a \LaTeX file prepared by the author.